

Temperature-Programmed Sulfiding of $\text{MoO}_3/\text{Al}_2\text{O}_3$ Catalysts

P. ARNOLDY,¹ J. A. M. VAN DEN HEIJKANT, G. D. DE BOK, AND J. A. MOULIJN

Institute for Chemical Technology, University of Amsterdam, Nieuwe Achtergracht 166, 1018 WV Amsterdam, The Netherlands

Received June 14, 1983; revised January 30, 1984

The conversion of oxides into sulfides has been studied by means of temperature-programmed sulfiding (TPS). In TPS the H_2S , H_2O , and H_2 concentrations are measured continuously during sulfiding with a $\text{H}_2\text{S}/\text{H}_2/\text{Ar}$ mixture, as a function of temperature. Application of TPS to $\text{MoO}_3/\text{Al}_2\text{O}_3$ hydrosulfurization catalysts leads to detailed information on the sulfiding rate and mechanism. Sulfiding of $\text{MoO}_3/\text{Al}_2\text{O}_3$ takes place at low temperature in comparison with bulk compounds (MoO_3 , MoO_2). The sulfiding mechanism is dominated by O–S exchange reactions. Elemental sulfur is formed by rupture of metal sulfide bonds and is reduced subsequently by H_2 . In fact, H_2 plays only a minor role in sulfiding at low temperatures. Particularly the “ H_2O content” of the catalysts influences the sulfiding rate to a large extent. “Wet” catalysts, in equilibrium with 3% $\text{H}_2\text{O}/\text{Ar}$ at room temperature, sulfide at very low temperature (typically 400–500 K). “Dry” catalysts, treated in Ar at 775 K, on the other hand, sulfide at relatively high temperature (600–700 K). This H_2O effect is explained tentatively by catalysis of O–S exchange by Brønsted acid sites. Prereduction hinders sulfiding more than predrying. This suggests a minor importance of reduced intermediates in normal sulfiding procedures. An increase in the Mo content (0.5–4.5 atoms/ nm^2) leads to sulfiding at lower temperature, but the influence of Mo content is not as pronounced as has been found in TPR reducibility studies. The influence of Mo content on TPR and TPS is explained by detailed consideration of the heterogeneity. Sulfiding of a 4.5 atoms/ nm^2 catalyst can be completed at ca. 500 K, up to a S/Mo ratio of 1.9, provided that a sufficiently low heating rate is chosen. The fact that such a low temperature is sufficient suggests the initial formation of monolayer-type sulfide species with a S/Mo ratio near 2. These species can exist if steric factors are taken into account. © 1985 Academic Press, Inc.

INTRODUCTION

$\text{Mo}/\text{Al}_2\text{O}_3$ catalysts can be used for various purposes. Among others they form an important building block for the commercially used hydrosulfurization (HDS) catalysts $\text{Ni-Mo}/\text{Al}_2\text{O}_3$ and $\text{Co-Mo}/\text{Al}_2\text{O}_3$. Many publications have centered on the preparation and structure of the oxidic form $\text{MoO}_3/\text{Al}_2\text{O}_3$ (1, 2). The reducibility of this oxidic form has been studied as a model for the overall reactivity of the surface oxides (3–5). Sometimes it has been possible to correlate reactivity of the oxidic catalysts with the HDS activity of presulfided catalysts. For instance, catalysts which reduce at the lowest temperature show the highest activity (5). Interpretation of this kind of

correlation is difficult because knowledge on the structure of sulfides and on the conversion of oxides into sulfides is limited. Relatively few studies have had the structure of the sulfided catalyst as their subject. However, recent *in-situ* measurements using Mössbauer emission spectroscopy and EXAFS have shed more light on the structure of the sulfided form (6, 7).

The actual process of sulfiding has also received little attention up to now (1, 8–11). Sulfiding is not understood in a fundamental way, although it is most important for achieving a high and stable HDS activity (12–15). Sulfiding is a necessary pretreatment for HDS catalysts in order to limit coke formation (16). Moreover, the study of sulfiding is important, because process control in large-scale presulfiding operations in commercial reactors is diffi-

¹ Present address: Koninklijke/Shell–Laboratorium, Badhuisweg 3, Amsterdam, The Netherlands.

cult, on account of the large exothermal effect of sulfiding reactions (14).

Some isothermal sulfiding experiments have been reported (9, 10). These measurements, however, were not able to elucidate sulfiding mechanisms in detail, for they were based only on overall sulfur analyses and detection of overall weight changes by means of a microbalance. Moreover, the isothermal measuring procedure does not give a realistic representation of normal sulfiding conditions; in practice sulfiding is started at room temperature and temperature is increased only gradually. Isothermal measurements are also not able to show the reactivity of all Mo species with respect to sulfiding: some species are sulfided fast and completely at the chosen temperature, while other species sulfide slowly or do not sulfide at all.

The objective of this study is to investigate the reactivity of oxidic Mo/Al₂O₃ catalysts with respect to sulfiding in H₂/H₂S mixtures. In our opinion the study of sulfiding in temperature programs is preferred to isothermal experiments. In this way normal sulfiding procedures can be simulated.

Moreover, in a single temperature-programmed sulfiding experiment the reactivity of all Mo species is registered: reactive species sulfide at low temperature, while less-reactive species sulfide at higher temperatures. This temperature-programming approach has already been successful in the characterization of reducibility of MoO₃/Al₂O₃ catalysts by means of temperature-programmed reduction (TPR) (5, 17).

In this study temperature-programmed sulfiding (TPS) (11) patterns will be presented of MoO₃/Al₂O₃ catalysts where the Mo content and the *in-situ* pretreatment have been varied. The TPS patterns give qualitative information on the sulfiding rate and the sulfiding mechanism as a function of temperature. Quantitative data can also be extracted from the TPS patterns to a certain extent. It will be shown that TPS is a sensitive technique able to describe sulfiding reactions in detail.

EXPERIMENTAL

a. Solid materials. Most p.a. chemicals (MoO₃, (NH₄)₆Mo₇O₂₄ · 6H₂O, α -S) did not show any X-ray diffraction (XRD) lines

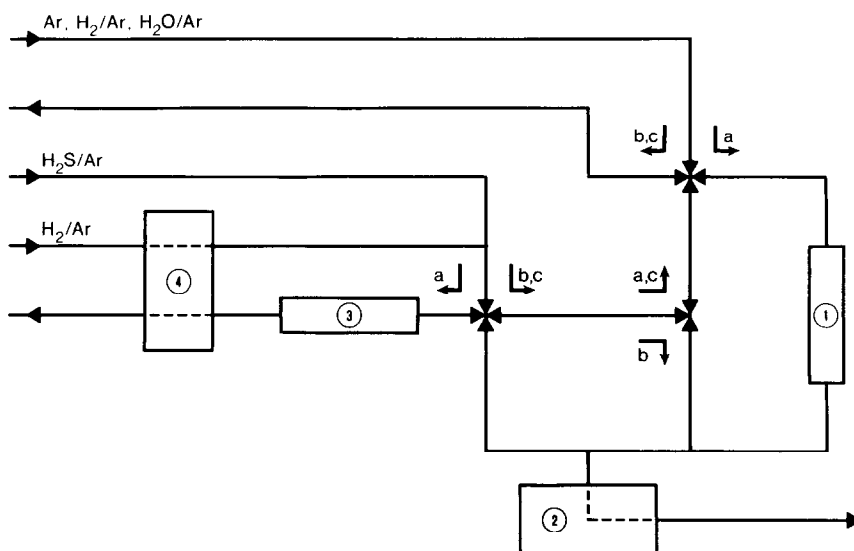


FIG. 1. Scheme of the TPS apparatus. 1, reactor; 2, mass spectrometer in UHV system; 3, molecular sieve column; 4, thermal conductivity detector. The arrows indicate the direction of the gas flow during (a) pretreatment, (b) stabilization of the mass spectrometer before sulfiding, and (c) sulfiding.

caused by impurities. Only MoO_2 (Ventron) showed low-intensity XRD lines of Mo metal impurity. For the catalyst preparation a Ketjen 000-1.5E high-purity $\gamma\text{-Al}_2\text{O}_3$ (CK-300) is used (specific surface area 213 m^2/g ; pore volume 0.51 cm^3/g ; particle size 180–300 μm). This support material was impregnated with aqueous ammonium heptamolybdate solutions, by means of the pore-volume impregnation technique. The impregnated solids were dried slowly in air, in a temperature program from 325 up to 395 K (heating rate 20 K/h) and isothermally at 395 K during one night. The dried samples were calcined in an air flow at 825 K for 2 h. The Mo contents, determined by means of atomic absorption spectrometry, were 2.3, 4.8, 9.9, and 18.6% MoO_3 by weight (i.e., 0.5, 1.0, 2.2, and 4.5 Mo atoms/ nm^2 , respectively). These catalyst samples have also been used in previous studies. In particular their HDS activity has been determined (675 K, thiophene) and their reducibility has been characterized by TPR (5, 17). Even at the highest Mo loading (4.5 atoms/ nm^2) no crystalline MoO_3 has been detected by means of X-ray diffraction or Raman spectroscopy.

b. In-situ catalyst pretreatment. All fresh samples were in equilibrium with the moisture in the air atmosphere at room temperature and lost ca. 6 wt% H_2O upon heating in air up to 385 K for 16 h. Before sulfiding all samples were pretreated *in situ* in several ways (each pretreatment took place for 30 min, if not stated otherwise):

- flushing in Ar at room temperature;
- vacuum (30 mbar) at 385 K for 16 h;
- flushing in Ar at 775 K;
- flushing in 3% $\text{H}_2\text{O}/\text{Ar}$ at room temperature;
- flushing in 69% H_2/Ar at 675 K (prereduction);

mixing physically with $\alpha\text{-S}$, followed by flushing in Ar at room temperature.

c. Temperature-Programmed Sulfiding (TPS). A simplified scheme of the TPS apparatus is shown in Fig. 1. The sample was held in a quartz tube (internal diameter 4–7

mm) between two quartz-wool plugs. The sample weight was varied in order to sulfide a constant amount of Mo per experiment (ca. 0.13 mmol Mo). The sulfiding mixture was prepared by mixing flows of 69% H_2/Ar (UHP quality, not further purified) and 5.84% $\text{H}_2\text{S}/\text{Ar}$ (UHP quality Ar, CP quality H_2S , purified by 3A molecular sieves). The flow rates were measured and controlled accurately with electronic flow controllers. The composition of the resulting gas mixture was 3.3% H_2S –28.1% H_2 –68.6% Ar (i.e., a pressure ratio $\text{H}_2/\text{H}_2\text{S}$ of 8.5). The total flow rate was ca. 11 $\mu\text{mol}/\text{s}$. The pressure in the reactor was ca. 1.05 bar. The sulfiding mixture was led continuously along a UHV unit containing a Riber QS 100B mass spectrometer. Via a leak valve a fraction of the mixture was pumped to the mass spectrometer (0.013 $\mu\text{mol}/\text{s}$, i.e., 0.1% of the total flow rate, at a UHV pressure of 2×10^{-6} mbar). The peak intensities of the masses (m/e) 2 (H_2), 18 (H_2O), 34 (H_2S), and 40 (Ar) were registered using a mass selector. One mass peak intensity was recorded per second; 99.9% of the gas mixture was passed through a 5A molecular sieve column (internal diameter 11 mm; length 450 mm). This column functioned as a buffer with respect to the H_2O and H_2S concentrations: varying concentrations of H_2O and H_2S at the outlet of the reactor were transformed to a constant concentration by passage through the molecular sieve. In this way variations in the thermal conductivity, measured after the molecular sieve, could be ascribed completely to changes of the H_2 concentration at the reactor outlet. The quartz tube containing the sample was installed in a furnace, which could be heated in linear temperature programs. The tubes between the reactor and the mass spectrometer were all heated at ca. 390 K, in order to avoid condensation of H_2O . Nevertheless, in the case of large H_2O production during TPS (400–800 mg samples) some H_2O still condensed in the leak valve, leading to a decrease of stability of the mass signals.

The TPS sulfiding experiments could be divided into three stages (see Fig. 1):

(a) The *in-situ* pretreatment: the pretreatment gas was flowing through the reactor, while, simultaneously, the sulfiding mixture was flowing through the molecular sieve and thermal conductivity detector.

(b) The sulfiding mixture was flowing along the mass spectrometer without passing through the reactor, in order to accustom the mass spectrometer to the H_2S medium and to measure the inflowing sulfiding mixture composition.

(c) The sulfiding mixture was flowing through the reactor; after a switch peak, i.e., an artificial H_2S consumption peak caused by the pushing aside of the pretreatment gases, sulfiding was registered. Sulfiding is divided in an isothermal sulfiding stage at room temperature and the actual temperature-programmed sulfiding stage. Sulfiding was registered at room temperature until the gas mixture had reached its original composition (within 1 h). Then the temperature was increased from room temperature up to 1270 K (with a heating rate of 10 K/min, unless stated otherwise), followed by an isothermal stage at 1270 K (30 min in general).

H_2S is not a very stable molecule. It can dissociate into H_2 and S_2 . This reaction, however, is suppressed for the most part by the presence of H_2 in the sulfiding mixture; H_2S conversion to S_2 is 0.4% at most, at 1270 K.

All parts of the equipment were made of corrosion-resistant materials. Nevertheless, corrosion still caused severe problems. For instance, every 20–30 experiments the mass spectrometer filament (W or 3% Re/W) had to be replaced.

Overall H_2S consumption during TPS could be calculated, with a standard deviation of ca. 10% in general. The H_2 consumption could be calculated from the thermal conductivity data. The stability of the thermal conductivity signal, however, was limited because of small variations in the gas composition as a consequence of

the mixing of two flows. Thus for calculation of H_2 consumption the standard deviation was also ca. 10%. H_2O mass signals have never been treated in a quantitative way, because a H_2O background concentration was always present in the UHV system and, moreover, H_2O production took place not only by Mo sulfiding but also by carrier dehydration.

d. *X-Ray Diffraction*. After TPS measurements the samples were cooled slowly to room temperature, in the sulfiding mixture. Subsequently the samples were exposed to air. In this way no severe oxidation of the sulfided samples could have taken place (18). The XRD patterns of the air-exposed samples were recorded. $\text{CuK}\alpha$ radiation was used; $\text{CuK}\beta$ radiation was removed by a Ni filter.

RESULTS

I. Temperature-Programmed Sulfiding

a. *Reference compounds*. In Fig. 2 the TPS patterns of the reference compounds MoO_3 and MoO_2 are shown. In this and in all following TPS figures the change of $p_{\text{H}_2\text{S}}$ corresponding to 50% conversion of H_2S is indicated with a double-headed arrow. Only the temperature-programmed part is given in Fig. 2, because no sulfiding is observed at room temperature. Nevertheless, for MoO_3 a color change is observed from greenish white to greyish blue during room-temperature sulfiding, which suggests a minor degree of sulfiding. The XRD pattern of MoO_3 after room-temperature sulfiding, however, shows only the original MoO_3 diffraction lines.

Sulfiding of MoO_2 takes place at very high temperature (above 950 K). H_2S is consumed, while H_2O is produced simultaneously; the H_2 concentration does not change. Sulfiding to MoS_2 is not completed at 1270 K. The H_2S uptake, at the end of the 1270 K isothermal stage, corresponds to a S/Mo ratio in the product of 1.4.

Sulfiding of MoO_3 is more complicated. Several features can be discerned. First of

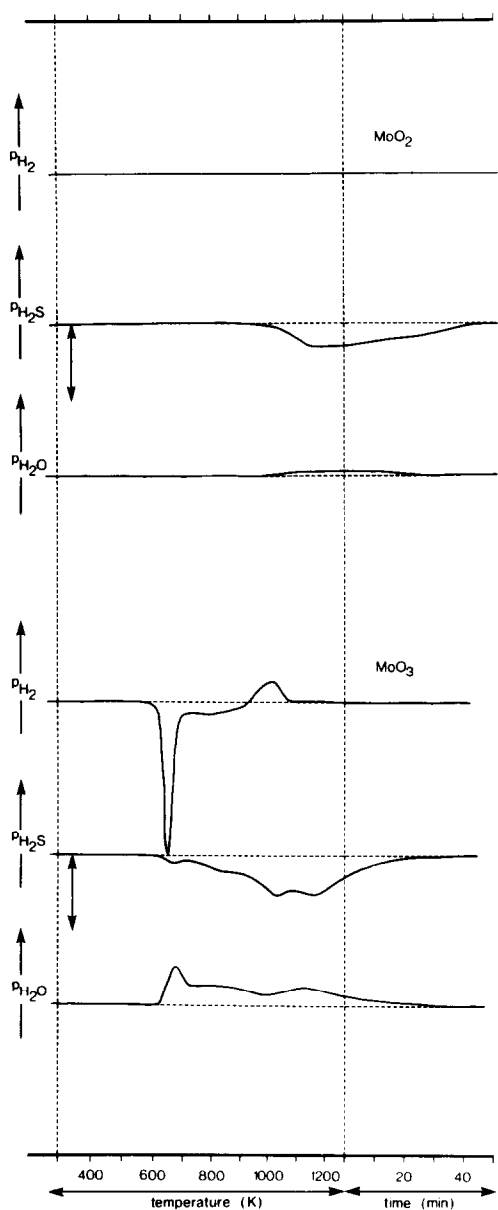


FIG. 2. TPS patterns (H_2S , H_2O , H_2) of the reference compounds MoO_2 and MoO_3 . The 50% conversion level of H_2S is indicated by a double-headed arrow.

all, at 650 K H_2 is consumed in a very sharp peak ($1.0 \text{ H}_2/\text{Mo}$) and simultaneously H_2O is produced. Also a minor amount of H_2S is consumed at 650 K. Between 700 and 1270 K the major uptake of H_2S takes place, in a very broad pattern. The sharp H_2 consumption peak is followed by a second reduction

peak at ca. 800 K ($0.15 \text{ H}_2/\text{Mo}$) and a H_2 production peak at 1020 K ($0.15 \text{ H}_2/\text{Mo}$). The H_2O production pattern follows the H_2 and H_2S patterns. The sulfiding to MoS_2 is almost completed in the isothermal stage at 1270 K. The XRD pattern of the product still shows traces of MoO_2 besides dominating lines of hexagonal MoS_2 , but the H_2S uptake corresponds to a S/Mo ratio in the product of 2.1.

b. $\text{MoO}_3/\text{Al}_2\text{O}_3$ catalysts. Quantitative TPS data, viz. the H_2S and H_2 consumption, are given in Table 1.

Figure 3 shows two typical TPS patterns of catalysts (4.5 atoms/nm^2 ; pretreated in Ar at room temperature and 775 K, respectively). Again only the temperature-programmed region is given, although in this case sulfiding at room temperature is measurable. The isothermal sulfiding stage at room temperature will be treated in the context of Figs. 5 and 6.

The catalyst TPS patterns are completely different from those of the reference compounds. Some H_2S evolution is observed just above room temperature (H_2S desorption), followed directly by H_2S consumption (320–450 K). H_2O is evolved in a pattern which is identical to the H_2S consumption pattern, but is shifted slightly to higher temperature. No H_2 consumption is found below ca. 400 K. Around 500 K H_2 is consumed in a relatively sharp peak, while simultaneously H_2S is produced. Also the H_2O production increases somewhat. At temperatures above ca. 550 K H_2S is consumed again, accompanied by H_2O production. Now also some H_2 consumption takes place (for the sample pretreated at 775 K), in contrast to what occurs in the low-temperature sulfiding region. The total H_2 consumption is ca. $1.0 \text{ H}_2/\text{Mo}$. The H_2S consumption is ca. 1.9 S/Mo . Dehydration of the support gives a background of H_2O production, up to very high temperatures.

The pretreatment of the catalysts influences the TPS patterns to a large extent. Pretreatment in Ar at 775 K, instead of at room temperature, leads to a shift of the

TPS pattern to much higher temperature and to a broadening of the TPS pattern. This phenomenon will be illustrated further in Figs. 5, 6, and 7.

Apart from the room-temperature sulfiding, from Fig. 3 three sulfiding regions can be discerned, viz.:

low-temperature sulfiding (below 500 K); H_2S is consumed, H_2O is produced;

H_2S production (400–550 K), coupled to H_2 consumption;

high-temperature sulfiding (above 500 K); H_2S is consumed and H_2O is produced, as in the low-temperature sulfiding region; some H_2 consumption takes place.

These three regions are present in the TPS patterns of most catalysts studied. For convenience in the following figures only the

H_2S concentration profile as a function of temperature will be given. H_2 and H_2O patterns are always related to the H_2S pattern, as in Fig. 3.

In Fig. 4 the influence of relevant experimental conditions on the TPS patterns is illustrated. TPS of 4.5 atoms/ nm^2 catalysts (flushed in Ar at room temperature) is shown using various heating rates (1 and 10 K/min) and sample weights (25, 100, and 200 mg). In a qualitative way, these TPS patterns have the same characteristics as shown in Fig. 3. Lowering the heating rate from 10 to 1 K/min leads to a shift of the TPS pattern to lower temperature, as is always found in temperature-programmed studies. It even seems possible to complete sulfiding up to a S/Mo ratio of ca. 2 at about

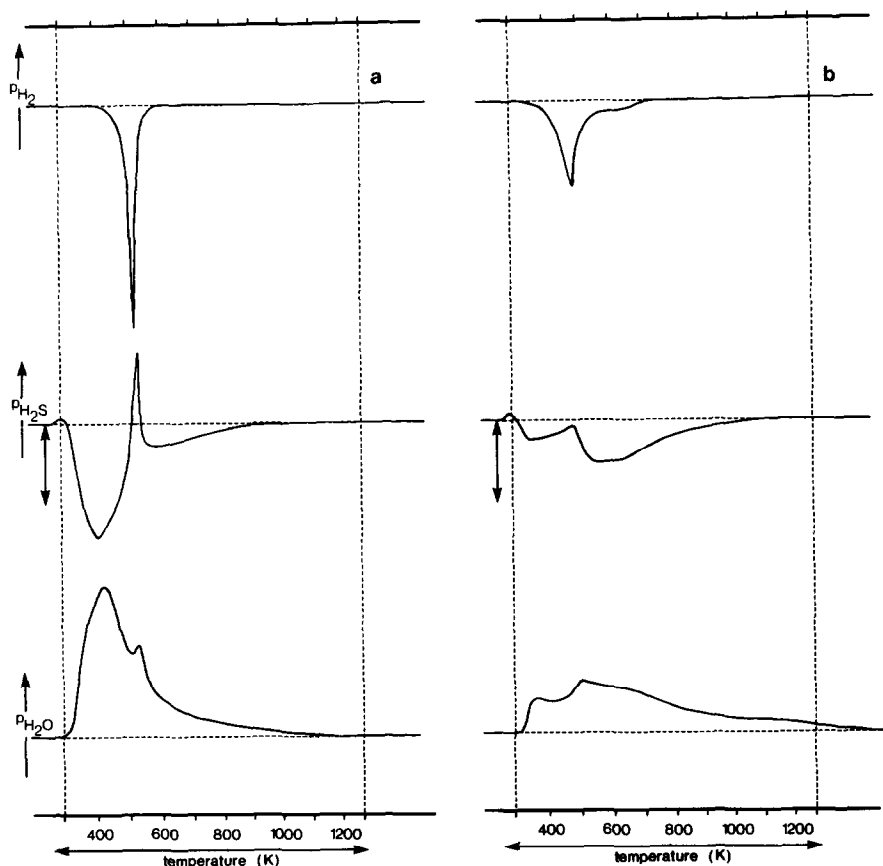


FIG. 3. TPS patterns (H_2S , H_2O , H_2) of $\text{MoO}_3/\text{Al}_2\text{O}_3$ (4.5 atoms/ nm^2 , 100 mg). (a) Pretreated in Ar at room temperature; (b) pretreated in Ar at 775 K. The 50% conversion level of H_2S is indicated by a double-headed arrow.

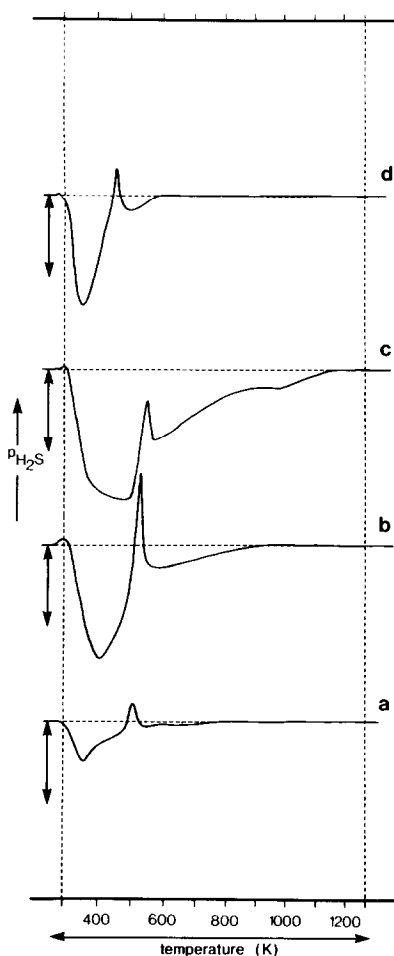


FIG. 4. TPS patterns (H_2S) of $\text{MoO}_3/\text{Al}_2\text{O}_3$ (4.5 at-oms/ nm^2), pretreated in Ar at room temperature; variation of sample weight and heating rate. (a) 25 mg, 10 K/min; (b) 100 mg, 10 K/min; (c) 200 mg, 10 K/min; (d) 500 mg, 1 K/min. The 50% conversion level of H_2S is indicated by a double-headed arrow.

500 K. The heating rate does not influence the shape of the TPS curve significantly. The influence of sample weight is more pronounced. An increase of sample weight from 25 to 100 mg leads to a small shift of the H_2S consumption peak (less than 50 K). The shape of the TPS peak is not affected severely. Using a sample weight of 200 mg the TPS pattern is deformed significantly and is shifted to much higher temperatures. Evidently the use of very large samples leads to integral H_2S conversion which can become so large that H_2S is consumed al-

most completely. In principle the use of small samples is preferred, in order to achieve differential conditions and simple kinetics. However, the accuracy of the measurements decreases for very small samples, because of limited stability of the mass spectrometer device. An increase of sample weight to ca. 100 mg is needed for increased sensitivity. For this sample weight (corresponding to 0.13 mmol Mo) integral conversions are reached, but no severe deformation occurs. Therefore all other TPS experiments have been executed with a constant amount of Mo of 0.13 mmol. In this way sulfiding never leads to more than 70% H_2S conversion.

Figure 5 gives TPS patterns of catalysts pretreated in Ar at room temperature. The isothermal sulfiding stage at room temperature is also shown. The unloaded support adsorbs a small amount of H_2S at room temperature, which is desorbed in the beginning of the temperature program. At 1120 K some H_2S is produced. Simultaneously, H_2O is produced and H_2 is consumed. Probably some sulfate or sulfite impurities are present in the support, which are reducible at 1120 K. H_2S consumption takes place for all catalysts at room temperature. This room-temperature sulfiding is completed essentially within 1 h. Catalysts adsorb much more H_2S than the unloaded support, as is evident for the low-loaded catalysts in particular. Within the Mo-loaded catalyst series the H_2S adsorption at room temperature per unit weight of the support is constant. H_2S uptake is 0.07 mmol $\text{H}_2\text{S}/\text{g Al}_2\text{O}_3$ for the unloaded support and 0.35 mmol $\text{H}_2\text{S}/\text{g Al}_2\text{O}_3$ for the Mo-loaded catalysts. For all catalysts color changes are observed at room temperature. The initially white color of the samples transforms fast to yellow, orange and brownish-orange, and more slowly to brown. The intensity of the color after 1 h sulfiding at room temperature varies with Mo content, from light brown for the 0.5 atom/ nm^2 catalyst to dark brown for the 4.5 atoms/ nm^2 catalyst. In a separate experiment room-temperature sul-

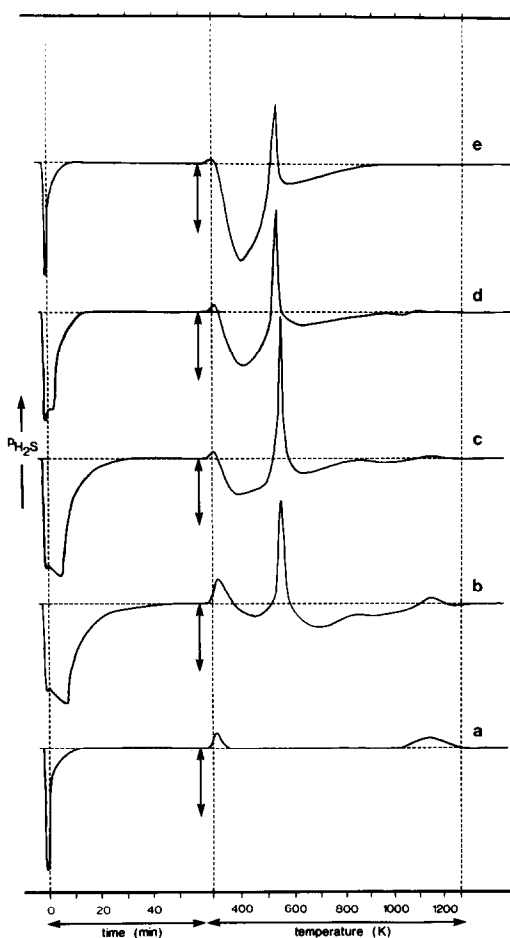


Fig. 5. TPS patterns (H_2S) of $\text{MoO}_3/\text{Al}_2\text{O}_3$ with varying Mo content, pretreated in Ar at room temperature. (a) 400 mg, 0 atoms/ nm^2 ; (b) 800 mg, 0.5 atom/ nm^2 ; (c) 400 mg, 1.0 atom/ nm^2 ; (d) 200 mg, 2.2 atoms/ nm^2 ; (e) 100 mg, 4.5 atoms/ nm^2 . The 50% conversion level of H_2S is indicated by a double-headed arrow.

fiding during 16 h led to a black instead of a brown color.

In the temperature program H_2S evolution occurs first (H_2S desorption), and this is larger for the catalysts with lower Mo content. The low-temperature sulfiding region is present for all catalysts, but is most important for the catalysts with high Mo content. The sharp H_2S production peak (coupled with H_2 consumption) is also observed for all catalysts. The position of this peak shifts as a function of Mo content; increase of the Mo content leads to a de-

crease of the peak temperature from 550 to 530 K. The high-temperature sulfiding region is always present and is more important for the catalysts with lower Mo content.

The overall H_2 uptake is 1.0 H_2/Mo , independent of Mo content (see Table 1). The H_2 consumption in the high-temperature sulfiding region decreases with Mo content. All other H_2 uptake is found in the sharp peak at ca. 500 K. The overall H_2S uptake increases with Mo content from 1.7 to 1.9 (see Table 1). The H_2S and H_2 uptake values are corrected for the H_2S production peak at 1120 K, which is attributed to the

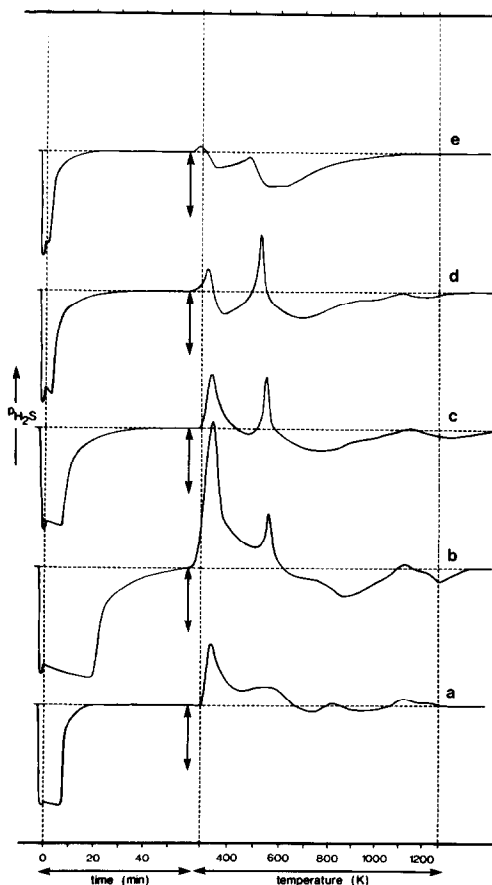


Fig. 6. TPS patterns (H_2S) of $\text{MoO}_3/\text{Al}_2\text{O}_3$ with varying Mo content, pretreated in Ar at 775 K. (a) 400 mg, 0 atoms/ nm^2 ; (b) 800 mg, 0.5 atom/ nm^2 ; (c) 400 mg, 1.0 atom/ nm^2 ; (d) 200 mg, 2.2 atoms/ nm^2 ; (e) 100 mg, 4.5 atoms/ nm^2 . The 50% conversion level of H_2S is indicated by a double-headed arrow.

TABLE 1

H₂S and H₂ Consumption in TPS, as a Function of Mo Content and *in-Situ* Pretreatment

Pretreatment	Mo content (atoms/nm ²)	H ₂ S/Mo ^a (mol/mol)	H ₂ /Mo ^b (mol/mol)	H ₂ /Mo ^c (mol/mol)
Ar flushing (room temperature)	0.5	1.7	0.65	0.35
	1.0	1.7	0.75	0.25
	2.2	1.7	0.9	0.1
	4.5	1.9	1.0	0.0
Ar flushing (775 K)	0.5	1.4	0.5	0.5
	1.0	1.6	0.55	0.45
	2.2	1.5	0.65	0.35
	4.5	1.8	0.8	0.2
H ₂ /Ar flushing (675 K)	4.5	1.9	0.0	0.0

^a Total H₂S consumption in TPS, corrected for Al₂O₃.^b H₂ consumption in the H₂S production peak at ca. 500 K.^c H₂ consumption in the high-temperature sulfiding region (>500 K).

support. In all cases Mo sulfiding appears to be completed at the end of the temperature program (1270 K).

Figure 6 gives the TPS pattern of catalysts pretreated in Ar at 775 K. Although all minima and maxima are present as in Fig. 5, the pattern shape is completely different. This is also observed for the 4.5 atoms/nm² sample in Fig. 3. Room-temperature H₂S uptake is more important than after pretreatment at room temperature and is much larger for the catalysts (0.7 mmol H₂S/g Al₂O₃) than for the unloaded support (0.35 mmol H₂S/g Al₂O₃). H₂S adsorption (at room temperature) and desorption (in the temperature program) are increased by the 775 K pretreatment in the same way. H₂S desorption now dominates the TPS patterns to such an extent that real sulfiding characteristics can hardly be discerned, especially at low Mo content. For all catalysts the low-temperature sulfiding region has become less important by pretreatment at 775 K, whereas the high-temperature sulfiding region has become more important. Some influence of the Mo content on the sulfiding rate can be observed. Catalysts with lower Mo content sulfide at higher temperature. The H₂S production peak shifts with increasing Mo content from 560 to 480 K. The

increased importance of the high-temperature sulfiding region is also observed as an increase of the H₂ consumption values in this region (see Table 1), with respect to the catalysts pretreated in Ar at room temperature. Again the distribution of H₂ consumption over the TPS regions is dependent on Mo content. The overall H₂S uptake increases with Mo content from 1.4 to 1.8 S/Mo (see Table 1).

Because the TPS patterns of catalysts are influenced by pretreatment significantly, pretreatment conditions have been varied more systematically. Typical results for the 4.5 atoms/nm² catalyst are given in Fig. 7.

The "H₂O content" (physically and chemically adsorbed H₂O) is varied in Figs. 7b–e. Figures 7c and e are also presented in Fig. 3. Figure 7b shows the influence of flushing with 3% H₂O/Ar at room temperature. Only slight differences can be observed with respect to Fig. 7c. A sample which is pretreated in Ar at 775 K and is flushed with 3% H₂O/Ar at room temperature afterwards, shows precisely the same TPS pattern as presented in Fig. 7b. The latter experiment proves that the H₂O content influences sulfiding and induces structural changes which are reversible. Also mild drying conditions (385 K *in vacuo*)

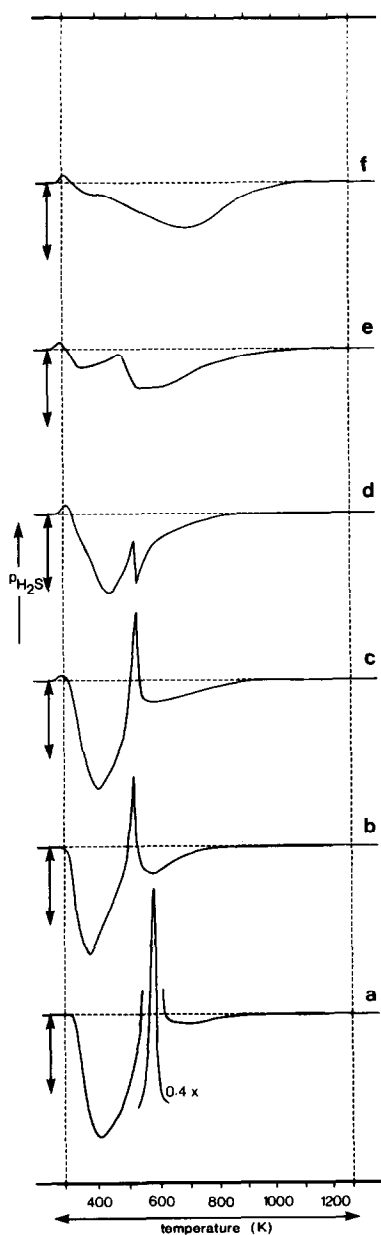


FIG. 7. TPS patterns (H_2S) of $\text{MoO}_3/\text{Al}_2\text{O}_3$ (4.5 atoms/ nm^2 , 100 mg) after different pretreatments. (a) Addition of elemental sulfur (1.7 S/Mo), followed by flushing in Ar at room temperature; (b) 3% $\text{H}_2\text{O}/\text{Ar}$ at room temperature; (c) Ar at room temperature; (d) vacuum at 385 K; (e) Ar at 775 K; (f) 69% H_2/Ar at 675 K. The 50% conversion level of H_2S is indicated by a double-headed arrow.

lead to changes in the TPS pattern (Fig. 7d). In fact, from Figs. 7b–e it can be observed that the TPS patterns change continuously

as a function of the H_2O content. Depending on H_2O content the catalysts will be referred to as “wet” or “dry.”

A reduction pretreatment at 675 K leads to a complete disappearance of the H_2S evolution peak at 500 K (Fig. 7f). No H_2 is consumed in this experiment. Only a very broad H_2S consumption band is left, comparable with the TPS high-temperature sulfiding region in the severely dried catalyst (Fig. 7e). However, the position of this band for the prereduced catalyst is shifted to even higher temperatures. The S/Mo ratio after TPS is 1.9 for this reduced sample.

One sample was mixed physically with an amount of elemental sulfur corresponding to 1.7 S/Mo. This addition leads to an intensification of the H_2S evolution peak, shifted to somewhat higher temperature (580 K) (Fig. 7a) and accompanied by a sharp increase of the H_2 consumption. Sulfur mixed with the unloaded support was not reduced in TPS; all added sulfur evaporated during TPS. It is therefore concluded that the reduction of sulfur is catalyzed by Mo sites.

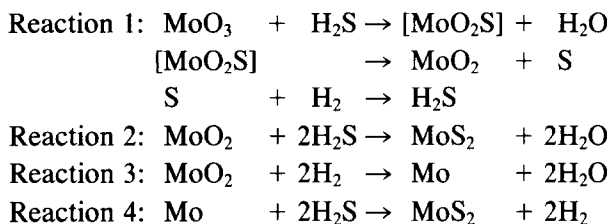
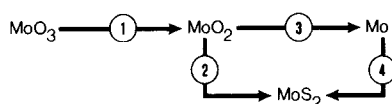
II. X-Ray Diffraction

The samples used in TPS measurements (exposed at 1270 K for 30 min) showed broad diffraction lines of $\delta\text{-Al}_2\text{O}_3$ of low intensity. For the 0.5 atom/ nm^2 catalyst no other diffraction lines were observed. For higher Mo contents weak diffraction lines of rhombohedral MoS_2 were observed. The intensity of these lines increased with Mo content. Even for the 4.5 atoms/ nm^2 catalyst, however, the MoS_2 lines were less intense than the $\delta\text{-Al}_2\text{O}_3$ lines.

DISCUSSION

I. TPS of Reference Compounds

The TPS patterns of MoO_2 and MoO_3 have led us to the sulfiding model shown in Scheme 1. This sulfiding scheme is in agreement with literature as far as Reactions 1 and 2 are concerned (8, 19–21). H_2S has been suggested as reducing agent in Reaction 1 (19, 20), for the reduction of MoO_3 to



SCHEME 1

MoO₂ is more rapid in the presence of H₂S and takes also place in the absence of H₂. Preliminary results of TPS using a sulfiding mixture of 2% H₂S/N₂ showed that indeed reduction of MoO₃ to MoO₂ takes place in the absence of H₂ by H₂S as reducing agent, precisely at the reduction temperature found in Fig. 2 (22). It follows from Fig. 2 that the effective H₂S consumption in Reaction 1 is small, while the main reactant is H₂, which is consumed rapidly (1 H₂/Mo). It is concluded that H₂S reduces MoO₃, via MoO₂S, to MoO₂ rapidly with production of elemental sulfur, which can be reduced immediately to H₂S by H₂ as can be seen in Fig. 7a for sulfur mixed with a 4.5 atoms/nm² catalyst. The proposed MoO₂S structure is not intended to exist as a bulk phase; it will only be present as an unstable intermediate on a molecular scale.

The fact that, in the attack of MoO₃, H₂S is more reactive than H₂ shows that O–S-exchange is an easier reaction than the Mo–O bond breaking involved in reduction by H₂ (23). Additionally, reduction by H₂ is much more hindered by H₂O, being reaction product, than sulfiding, since in the former case H₂O poisons catalytic centers needed for H₂ dissociation (23).

Simultaneously with Reaction 1 formation of MoS₂ starts via Reaction 2. However, at 650 K MoS₂ formation is slow and is limited to surface layers (19). Bulk sulfiding to MoS₂ takes place only at very high temperature showing the resistance of MoO₂ to sulfiding. Nevertheless, the MoO₂

formed *in situ* from MoO₃ sulfides more rapidly and more completely than the starting material MoO₂ (20). Probably the *in-situ* formed MoO₂ is more porous, so diffusion limitations for H₂S (19) are smaller and reaction can take place at lower temperature. H₂S diffusion limitations appear to be absent in the fast reduction of MoO₃ to MoO₂, so around 650 K probably a very open, porous MoO₃/MoO₂ system exists, whereas around 800 K the formed MoO₂ becomes much less porous.

For more than 15% of the Mo atoms sulfiding of MoO₃ to MoS₂ takes place via Mo metal as intermediate (Reactions 3 and 4). Literature reports show that metallic Mo is sulfided easily to MoS₂ at 900 K (20), in agreement with Reaction 4 found in TPS. Reduction of MoO₂ to Mo metal in H₂S/H₂ medium has not been reported before. Clearly there is a competition between H₂ and H₂S in the attack of the slightly porous MoO₂. It is concluded that H₂ wins the competition below ca. 900 K, due to a molecular-sieve effect. Sulfiding by H₂S dominates over reduction by H₂ only above ca. 950 K.

II. TPS of Catalysts

The sulfiding behavior of the reference compounds and the catalysts is completely different. Whereas MoO₃ is resistant to sulfiding up to ca. 600 K, the catalysts start sulfiding at much lower temperature. This can be explained by assuming that only surface Mo ions are sulfided easily. The obser-

vation that room-temperature sulfiding of MoO_3 led to a greyish blue color shows that also in this case sulfiding of minor amounts of surface ions (creating Mo(V) ions) is a fast reaction. In bulk MoO_3 , however, most ions are locked in a crystal lattice and are not accessible at low temperature. On the other hand, sulfiding of catalysts is not hindered at all, because dispersion of $\text{MoO}_3/\text{Al}_2\text{O}_3$ catalysts is reported to be complete up to a monolayer coverage of ca. 5 atoms/nm² (17, 24, 25).

a. Sulfiding reactions. Different sulfiding reactions take place in different temperature regions. The observation of these reactions, however, is hindered by H_2S adsorption/desorption phenomena. The latter will therefore be discussed first.

Most H_2S consumed at room temperature is adsorbed physically, as can be seen from H_2S desorption characteristics in the beginning of the temperature programs. It is surprising that the H_2S adsorption is ca. 0.3 mmol $\text{H}_2\text{S}/\text{g Al}_2\text{O}_3$ larger for the Mo-loaded catalysts than for the unloaded support. Apparently the addition of Mo ions to the support leads to formation of specific Mo sites. A priori, it would be expected that the amount of H_2S adsorbed increases with the Mo content. The fact that this amount is constant in the Mo-loading range studied (0.5–4.5 atoms/nm²) implies that the number of strong H_2S adsorption sites increases sharply with increasing Mo content below a Mo loading of 0.5 atom/nm². Therefore it can be calculated that 2 $\text{H}_2\text{S}/\text{Mo}$ or more adsorb on these sites. The adsorption of H_2S on specific sites might be explained by dissociative adsorption on Al_2O_3 (26), assisted by hydrogen bonding to neighboring Mo sites. In our opinion a better explanation might be that H_2S adsorption takes place selectively on Mo ions in a specific surrounding, and these are only present in low concentrations. TPR results show a strong influence of Mo content on reducibility: especially catalysts with low Mo content are hardly reducible in comparison with crystalline MoO_3 and catalysts

with high Mo content (5, 17). TPR results thus point also to a specific surrounding of Mo at low Mo content. This can be pictured as follows. In Mo oxides Mo–O bonds are quite covalent (27). Presence of Al ions in the Mo surrounding will polarize these bonds, leading to a larger effective charge on Mo and increased Coulomb interactions. This effect is often described as strong interaction between metal ions and support. Especially at low Mo contents the polarization of Mo–O bonds will become large by surrounding with several Al ions. This will lead to low reducibility in TPR and strong electron deficiency on Mo ions, i.e., good H_2S adsorption properties.

In the following the sulfiding reactions will be discussed per temperature region.

(i) Low-temperature sulfiding. The observation of color changes during room-temperature sulfiding gives evidence for formation of Mo–S bonds. Most of these correlate well with the color changes found for reactions of Mo(VI) ions with H_2S in aqueous solution (28): MoO_4^{2-} (white) \rightarrow $\text{MoO}_3\text{S}^{2-}$ (yellow) \rightarrow $\text{MoO}_2\text{S}_2^{2-}$ (orange) \rightarrow MoOS_3^{2-} (orange-red) \rightarrow MoS_4^{2-} (red). The brownish color found for the catalysts is also found for bulk MoS_3 (29). Nevertheless, the amount of Mo–S bonds formed at room temperature is small.

In the low-temperature sulfiding region (below 500 K) as a whole H_2S consumption is significant and correlates well with H_2O production (see Fig. 3). No H_2 is consumed in this region. This shows that sulfiding occurs by simple O–S exchange on Mo(VI). It has been reported that Mo(IV) and Mo(V) are formed already at 423 K (8). In this study it is found that prolonged sulfiding at room temperature yields black samples, indicating the presence of reduced Mo ions. This reduction reaction can only take place by solid-state reactions, because no changes in the H_2 concentration have been observed in this region. Only rupture of Mo(VI)–S bonds with formation of elemental sulfur can explain the formation of reduced Mo ions.

(ii) *Reduction of surface sulfur.* At ca. 500 K H_2S is produced in a sharp peak, coupled to consumption of H_2 . Sometimes the H_2S concentration even exceeds the inflowing H_2S level! Apparently some surface sulfur species is reduced. The sharpness of the peak points to a chemically well-defined surface compound. Addition of elemental sulfur (see Fig. 7a) leads to a drastic increase of H_2S production and H_2 consumption. This observation proves that sulfur can be reduced in this temperature region and is a strong indication that the reaction at 500 K in TPS is reduction of sulfur. Thus it is concluded that sulfur is formed during sulfiding at temperatures below 500 K by breaking of Mo(VI)-S bonds. The presence of free sulfur has already been reported. At least part of the sulfur is present as a paramagnetic sulfur species, as detected by ESR (30). Also instability of Mo(VI)-S bonds is reported in the case of MoS_3 (29, 31, 32). MoS_3 , if it does exist, decomposes at quite low temperature (475–675 K) to initially amorphous MoS_2 and elemental sulfur (32).

Formation of sulfur is not detected in the TPS equipment directly, because sulfur will be adsorbed strongly to the support and consequently sulfur formation will not change the gas composition.

The sulfur formation appears to be a process that is catalyzed by Mo sites. The shift of the H_2S peak to higher temperature after sulfur addition (see Fig. 7a) can be understood if it is assumed that some inhibition of the catalyzed reduction occurs, e.g., by sulfur itself. Also the variation in peak temperature as a function of Mo content and pretreatment can be explained by this catalyzed reduction concept. A decrease of Mo content leads to a decrease of activity for sulfur reduction per Mo site, which is observed as an increase of the H_2S peak temperature. A drying pretreatment increases the sulfur reduction rate (see Fig. 3), probably because drying leads to an increase of coordinatively unsaturated sites. The extreme sharpness observed in most

cases for the H_2S peak suggests that the number of these sites increases fast as a function of temperature, e.g., by H_2O desorption.

The H_2 consumed in the peak at 500 K corresponds with reduction of 0.5–1.0 mol sulfur atoms per mol Mo, the exact amount depending on the Mo content and pretreatment. Apparently most Mo ions are reduced at low temperature to mainly Mo(IV) , by a sequence of sulfiding by O–S exchange and breaking of Mo(VI)-S bonds, accompanied by formation of elemental sulfur. Rupture of individual Mo(VI)-S bonds will reduce Mo(VI) to Mo(IV) in one step. However, it has been reported that small amounts of Mo(V) are present as an intermediate during sulfiding (1, 8). This can be explained assuming that some sulfur is removed from Mo(VI)-S-Mo(VI) bridged structures, leading to two Mo(V) ions per sulfur atom removed.

In the H_2S production peak at 500 K 0.5–1.0 mol H_2S per mol Mo is expected to be evolved, corresponding with the H_2 consumption of 0.5–1.0 H_2/Mo . Nevertheless, the H_2S peak is much smaller than expected, especially at high Mo content. Probably the H_2S production at 500 K is masked by rapid reactions which consume H_2S simultaneously, by O–S exchange. These sulfiding reactions will be accelerated because the H_2S concentration can become very large within the pores, as a result of sulfur reduction. This acceleration can be seen directly in TPS as an increase of the H_2O production (see Fig. 3).

The role of H_2 is very limited at low sulfiding temperature. It is concluded that, if sulfiding takes place at low temperature for sufficiently long periods (see Fig. 4d), it is possible to reach the end stage of sulfiding in the low-temperature sulfiding region, without any interference of H_2 . Then, after H_2S uptake is complete, H_2 is consumed in order to remove the adsorbed elemental sulfur. In the literature a competition between H_2S and H_2 is often proposed in the attack on the oxidic catalysts (15, 21). This

study shows this is not the case at low sulfiding temperature, where H_2S predominates in sulfiding via O-S exchange. This is confirmed by TPS experiments using a 2% $\text{H}_2\text{S}/\text{N}_2$ sulfiding mixture, which showed H_2S consumption patterns comparable with the TPS patterns presented here, as far as the low-temperature sulfiding region is concerned (22).

(iii) *High-temperature sulfiding.* In this region (above 500 K) sulfiding is completed. The overall H_2 consumption in TPS is 1 H_2/Mo , corresponding to the reduction of Mo(VI) to an average valency of (IV).

Above 500 K, H_2S consumption is coupled again to H_2O production. Now also some H_2 is consumed, due to completion of Mo reduction to Mo(IV). Most Mo ions, however, are already in the Mo(IV) state in the beginning of the high-temperature sulfiding region. Thus it is concluded that sulfiding in this region can be described mainly as O-S exchange on Mo(IV) ions. In some sulfiding reactions H_2 plays a role. Direct reduction of Mo(VI) to Mo(IV) by H_2 cannot be excluded on the basis of TPR results (5, 17). However, it is also possible that the same sulfiding sequence takes place as in the low-temperature sulfiding region: H_2 is consumed in sulfur reduction, being a very fast reaction above 500 K.

Some contradiction is found in the literature on the Mo valency after sulfiding. Most authors agree on the presence of Mo(IV) after sulfiding at ca. 675 K (25, 33). Only minor amounts of Mo(III) and Mo(V) have been traced by ESR (34). Massoth, however, reports Mo(IV) formation to be far from complete up to very high temperature (9). Since some H_2O desorbs only at a very high temperature (see Fig. 3), perhaps in his measurements with a microbalance strongly adsorbed H_2O interfered.

A Mo(IV) phase as a result of complete sulfiding is reasonable on thermodynamic grounds. Mo(IV) occurs in crystalline MoS_2 , which is the stable Mo-S phase over a large range of temperatures and $\text{H}_2/\text{H}_2\text{S}$ pressure ratios (32). Hence it is not surpris-

ing that Mo(IV) is found in TPS as the stable ion in the presence of sulfide ligands, also in more dispersed phases.

H_2S consumption by Mo surface ions appears to be completed at high temperature (ca. 1100 K). Experimental S/Mo ratios are all slightly below 2 after TPS up to 1270 K. These values are essentially in agreement with literature values for sulfiding at ca. 675 K (10, 12, 25, 35). Apparently the removal of Mo-related oxygen ions is not complete, even after sulfiding at 1270 K! Especially at low Mo content the S/Mo ratio is smaller, so oxygen ions are left in the coordination sphere of Mo(IV) ions, showing the stability of some Mo(IV) oxide or oxysulfide surface species. At high Mo content the S/Mo ratio approaches 2, which implies formation of an almost stoichiometric MoS_2 phase for high Mo content.

b. Influence of the Mo content. All TPS patterns are the result of both sulfiding and adsorption/desorption of H_2S . At low temperature these processes take place simultaneously. Especially at low Mo content the adsorption and desorption phenomena dominate to such an extent that detailed analyses, e.g., accurate determinations of S/Mo ratios, are difficult. Qualitative conclusions also have to be made with care. For instance, in the interpretation of TPS patterns, it has to be taken into account that H_2S adsorbed at room temperature is used partly in the sulfiding reactions at low temperature. If one does so, the effect of Mo content on sulfiding rate is measurable, but small. Independent of the pretreatment it is found that the position of the TPS consumption bands is influenced by Mo content. Sulfiding takes place at higher temperature and is less complete for lower Mo contents. Also the H_2 uptake occurs for a larger part in the high-temperature sulfiding region for lower Mo contents. These observations reflect the variety in reactivity of different Mo ions and are in agreement with the concept of heterogeneity of the interaction of Mo ions in an oxidic surrounding with the Al_2O_3 support (4, 17, 24). Also the

very broad H_2S consumption bands in TPS point to a heterogeneous behavior of Mo ions.

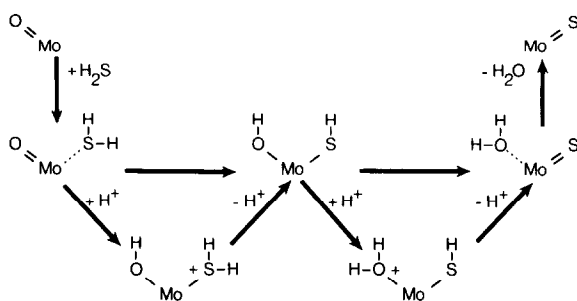
Heterogeneity can be interpreted as follows. Interaction with the support increases the Mo–O bond strength. An increase of Mo content (up to a monolayer coverage) leads to a gradual decrease of the average Mo–O bond strength, as has been illustrated by means of TPR studies (5, 17) (see also the discussion on H_2S adsorption at room temperature). The influence of coordination number of Mo ions on the Mo–O bond strength is probably small, because no typical TPR peaks for octahedrally or tetrahedrally surrounded Mo ions are observed. The differences in Mo–O bond strength can also explain changes in sulfiding rate. However, the influence of Mo content on sulfiding (TPS) is much less pronounced than on reduction (TPR). The influence of heterogeneity seems to be masked in sulfiding measurements. This can be explained tentatively, via an activation energy consideration. In general the activation energy of a reaction reflects partly the enthalpy difference between beginning and end state. In the case of TPR, the product of reduction is metallic Mo, having almost no interaction with the support. Thus the activation energy for reduction is mainly a function of the enthalpy of the beginning state: variations in support interaction (Mo–O bond strength) with Mo content will lead to a change of activation energy and, consequently, of reducibility. In sulfiding, on the other hand, the Mo–O bond rupture is accompanied by formation of a Mo–S bond (O–S exchange), which still interacts with the support considerably. Now variations in support interaction (Mo–O- and Mo–S bond strengths) with Mo content will change the enthalpy levels of beginning and end state in a similar way, so the enthalpy difference will not change to a large extent. This reasoning explains that the activation energy for sulfiding and the sulfiding rate will be only slightly dependent on Mo content, as found in TPS.

c. Influence of drying. The H_2O content of the oxidic catalysts has a drastic influence on sulfiding. Apparently structure changes are induced, which are reversible. Wet catalysts are sulfided easily, at low temperature. Dried catalysts show a much lower reactivity with respect to H_2S .

There has been one earlier attempt to study sulfiding in a temperature program (11). These authors gave one TPS pattern of a $\text{CoO-MoO}_3/\text{Al}_2\text{O}_3$ catalyst, which was dried previously (Fig. 6 of Ref. (11)). Their H_2S consumption pattern is quite similar to those presented in this study for dried catalysts (see Fig. 6). Their H_2O detection, however, appears to be retarded (see Fig. 3), probably caused by H_2O adsorption in cold tubes between the reactor and the detection device. The method these authors used for gas-phase analysis (gas chromatography) is too slow to follow reaction rate profiles (as the sharp H_2S production peak at 500 K) in temperature programs accurately.

The effect of H_2O can be explained assuming the O–S exchange in sulfiding is a proton-catalyzed surface reaction. It is well known that Mo catalysts contain large amounts of Brønsted acid sites (37), whereas drying leads to a sharp decline in the Brønsted acidity and an increase of Lewis acidity (38). It is assumed that proton transfer is the rate-determining step in the O–S exchange. If *intramolecular* proton transfer is slow, then an increase of the proton concentration on the neighboring surface will accelerate the reaction rate via *intermolecular* proton transfers. This is shown in Scheme 2.

The influence of H_2O on sulfiding rate has hardly been recognized in the literature. H_2O additions to catalysts before sulfiding have been claimed to improve catalyst activity for HDS (39). In that case extremely large amounts of H_2O were added: 20–120% of the pore volume, corresponding with ca. 10–60 wt% H_2O (assuming a pore volume of 0.5 ml/g). These authors ascribe H_2O as a solvent which is able to dissolve



SCHEME 2

the oxidic Mo surface species at low temperature, so a more rapid and more complete sulfiding is achieved by a better contact between H_2S and the Mo species in the aqueous phase. Our study shows that also much smaller amounts of H_2O , which will not be present as a liquid phase, lead to the same effect on sulfiding rate. Hence a role of H_2O as a solvent is improbable on the basis of our work.

Control of the H_2O content of catalysts might be important, especially for commercial large-scale presulfiding operations. When the sulfiding rate is not under control, the heat produced in the exothermal sulfiding reactions can generate hot spots (14). From our work it follows that the H_2O content of the oxidic catalysts is one of the most important parameters in the determination of the sulfiding rate. One may predict that manipulation of the H_2O partial pressure during sulfiding will also influence Brønsted acidity and consequently the sulfiding rate. A controlled slow sulfiding reaction at low temperature, leading to complete sulfiding, is required to reach optimum activity and stability (15). Therefore a good sulfiding procedure might be the following:

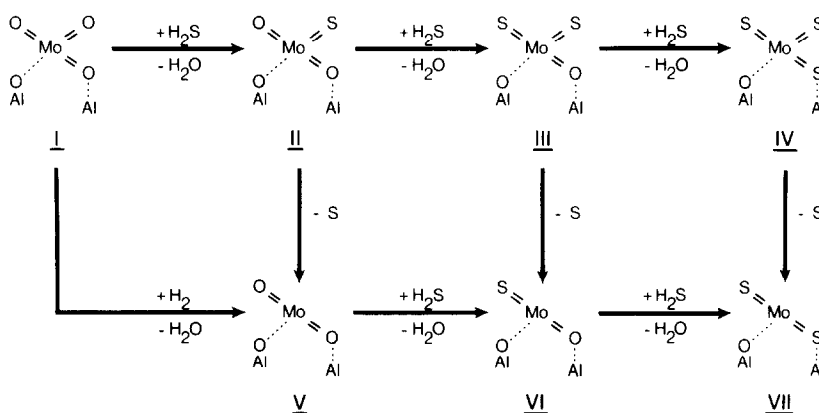
- (i) start sulfiding on a dried catalyst at 300–400 K;
- (ii) add H_2O in increasing concentrations to the gas phase at ca. 400 K;
- (iii) finally, increase the sulfiding temperature up to ca. 500 K, in order to complete sulfiding.

d. Influence of prereduction. The degree

of prereduction can be estimated from the TPS pattern. No H_2 is consumed or produced during TPS; also the H_2S peak at 500 K is absent. It is concluded that already during prereduction an average Mo valency of (IV) is reached, because only in that case does sulfiding require no further reduction or oxidation reactions to create the Mo(IV) sulfide product. Mo(III) and Mo(V) can occur only in minor amounts under our reduction conditions (3).

Prereduction has a large influence on sulfiding, as has been reported previously (9, 10, 21). One has to keep in mind that a reduction pretreatment also includes drying and removal of Brønsted acid sites (38, 40). However, TPS shows that the effect of prereduction on sulfiding is even more pronounced than the effect of drying alone. The very low sulfiding reactivity of reduced Mo catalysts suggests that the reduced Mo species is not identical to one of the reactive intermediates present in direct sulfiding of Mo(VI) species.

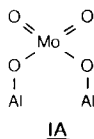
e. Mechanism of low-temperature sulfiding. Prior to TPS a monolayer of oxidic Mo ions is present in structures which are stabilized by strong interaction with the Al_2O_3 support (1, 5, 17). It is often suggested that during sulfiding this monolayer breaks up with formation of MoS_2 crystallites (21, 25, 41) or MoS_2 plates (6, 7). However, detailed knowledge on the mechanism of this sintering to MoS_2 particles is not available. In any case sintering to MoS_2 particles must be a subsequent reaction to the formation of well-dispersed MoS_2 . Thus it is relevant to



SCHEME 3

describe a mechanism for the formation of well-dispersed monolayer MoS₂. It is suggested that, at least at low temperatures (400–500 K), sulfiding takes place without severe distortion of the monolayer conformation. This low-temperature sulfiding is represented in Scheme 3.

To start with, monomeric tetrahedrally surrounded Mo ions are taken as model Mo surface species. The Mo(VI) ions have been coupled to the support by means of impregnation and calcination, via condensation reactions in which one or two OH groups of the support are involved (24, 42–44). The resulting Mo monolayer is often represented as



This structure suggests that two equivalent Mo–O double bonds and two equivalent Mo–O–Al groups are present. However, the results of this study show that a Mo(IV) sulfide is formed from a Mo(VI) oxide, so in sulfiding three oxygen ions are removed per Mo ion. Therefore a slightly modified structure I is proposed, with three double Mo–O bonds (which have not to be equivalent) and a fourth oxygen ion, bonded strongly to the Al surface ion. Interaction between Mo oxide and support is shown by dotted lines. The Mo ion interacts with two Al ions, via

the Al–O group and a coordinatively unsaturated Al ion. All electrons are located in specific bonds for the sake of simplicity. In fact oxidic Mo compounds have a complicated electronic structure, which has both ionic and covalent features (27).

Structure I can be sulfided to a Mo(IV) surface oxysulfide with a S/Mo ratio of 2 (structure VII). At least for high Mo contents structure VII will be the sulfiding product for most Mo ions. Only in the case of very strong interaction with the support, at lower Mo contents, have lower S/Mo ratios been found, suggesting also structure VI as sulfiding product. In this case some very strong Mo–O bonds are left, which are not reactive with respect to sulfiding. The reaction pathway I → II → III → IV shows the O–S exchange on Mo(VI). The route V → VI → VII shows the O–S exchange on Mo(IV). The reactions II → V, III → VI and IV → VII show the reduction of Mo(VI) to Mo(IV) by rupture of one Mo(VI)–S bond.

Structure V has already been described as the result of moderate reduction in H₂ medium (4, 45). Structure VI has a S/Mo ratio of 1 and has been proposed as sulfiding product after procedures aimed at incomplete sulfiding (12, 25).

The main route of normal sulfiding will not go via intermediate V, because this structure appears to be sulfidable only at very high temperatures (see Fig. 7f). Hence

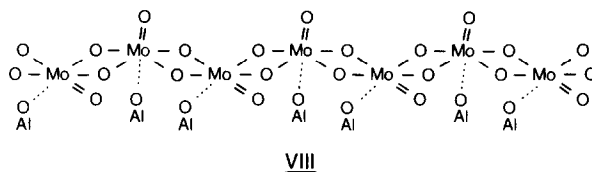
the main route of sulfiding will go from **I**, via **II** and **III**, to **VII**. Either structure **IV** or structure **VI** has to be intermediate in sulfiding. On the basis of this TPS work alone these intermediates are favored equally. However, consideration of steric factors (sulfide ions are larger than oxide ions) might lead to indications on the most likely reaction pathway.

The presence of more than one sulfide ion in the surrounding of Mo ions is proven to be possible for free Mo(VI) ions in aqueous solution (28). In fact MoS_4^{2-} can be the end product of sulfiding of MoO_4^{2-} ions in aqueous solution at room temperature. However, the more sulfide ions enter the Mo surrounding, the lower the sulfiding rate becomes (28), indicating increasing steric hindrance as sulfiding progresses.

In the case of catalysts, in some intermediates steric strain can be very important, especially in structure **IV** and to a smaller

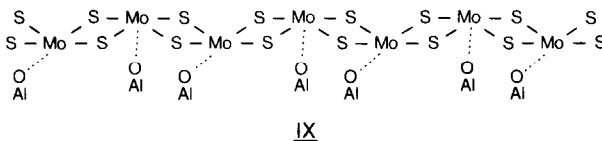
extent in structure **III**. Structure **III**, once formed, is expected to be not very stable, because of steric interactions of sulfide ligands in the capping layer. The reaction **III** \rightarrow **IV** leads to a further increase of steric strain and therefore is expected to be slow. The reaction **III** \rightarrow **VI**, however, leads to loss of steric strain by means of loss of elemental sulfur and therefore will be the favored pathway. So the most probable sulfiding route is **I** \rightarrow **II** \rightarrow **III** \rightarrow **VI** \rightarrow **VII**.

The structures **I** up to **VII** are too simple to model the sulfiding of $\text{MoO}_3/\text{Al}_2\text{O}_3$ catalysts. The proposed tetrahedrally surrounded Mo monomers are only present at low Mo surface coverages. At higher Mo contents more octahedrally surrounded Mo species occur, often aggregated into polymeric structures (1, 9, 18, 24, 46, 47). A possible structure is structure **VIII**. The oxidic Mo polymers are depicted as chains of octahedrally surrounded Mo ions:



Sulfiding of structure **VIII** is assumed to proceed via intermediates similar to those presented in Scheme 3 to a Mo(IV) sulfide

surface species with a S/Mo ratio of ca. 2 (structure **IX**) consisting of chains, in analogy with the oxidic structure **VIII**:



The transformation from **VIII** to **IX** will go via a series of O–S exchanges. The removal of sulfur from the polymer can lead to Mo(V) ions, as reported in the literature (1, 8). In structure **IX** the attachment to the support is still present via Al–O groups. Six-coordinated Mo(VI) ions transform into

five-coordinated Mo(IV) oxysulfide surface structures.

During the final stage of preparation of this article, an interesting *in-situ* Raman spectroscopic study on sulfiding of $\text{MoO}_3/\text{Al}_2\text{O}_3$ has been published (48). In this study Raman spectra are presented showing that

during sulfiding oxysulfides are involved as intermediates. Moreover, the authors conclude that sulfiding results in the formation of "MoS₂ surface layers" being highly reactive, disordered sulfides, which are bound extensively to the alumina by Mo–O–Al bonds. Their "MoS₂ surface layers" are similar to structures like **IX** presented in this study.

In the literature the existence of a completely sulfided monolayer has been rejected, mainly using the large radius of the sulfide ion as an argument (2, 43). The ionic radius of S²⁻ is 184 pm. Comparison with the ionic radius of O²⁻ (140 pm, which is also valid for the Al₂O₃ support) shows that sulfide ions are ca. 31% larger than oxide ions (49a). However, from the lattice parameters of MoS₂ crystallites a much smaller radius of S²⁻ can be calculated: 158 pm (32). Apparently the sulfide ions in the surrounding of Mo(IV) ions are not completely ionic and the sulfide radius is influenced by the environment to a large extent (49b). The value of 158 pm seems to be a better value for the S²⁻ radius in sulfided MoO₃/Al₂O₃, for it is calculated from a realistic lattice. Moreover, recently EXAFS data have shown that in sulfided MoO₃/Al₂O₃ the Mo–S distance is similar to the one in MoS₂ crystallites (7). Consequently, it is concluded that the S²⁻ radius is only 13% larger than the O²⁻ radius of the support. Thus it is necessary to reevaluate the implications of the steric-hindrance argument for the existence of monolayer structures.

Starting from a sulfide radius of 158 pm, a maximum density of 11.6 S atoms/nm² in a closest packed layer of sulfide ions can be calculated. In a monolayer (5 Mo atoms/nm²) which is sulfided completely (S/Mo ratio of 1.9) the surface coverage with sulfide ions is 9.5 S atoms/nm². Thus, if all sulfide ions are assumed to be in the same "capping layer," there is just enough space on the surface to accommodate a completely sulfided monolayer. Moreover, the sulfide ligands do not have to reside in the same

capping layer necessarily, because in sulfiding also the oxygen ions in the surface layer are removed. It is quite possible that sulfide ions become part of different layers. In this way the steric strain in the monolayer is relieved. Also the coordination number in the sulfided state (structure **IX**) is smaller than in the oxidic state (structure **VIII**), so the Mo–S bonds can bend away from the support somewhat, leading again to relief of strain. It is concluded that in principle a full monolayer of Mo oxysulfides can exist, taking into account the steric arguments.

In this study Mo oxysulfide species with a S/Mo ratio near 2 are presented tentatively as the product of low-temperature sulfiding (below ca. 500 K). However, these species might not be representative for the active species present on a sulfided MoO₃/Al₂O₃ catalyst under the corrosive practical HDS conditions (ca. 650 K, over long periods). Generally it is supposed that well-dispersed species decompose with formation of MoS₂ crystallites or two-dimensional MoS₂ sheets. It will be shown in a separate article (50) that from a combination of TPR, TPS, and HDS activity results evidence can be obtained for the presence of significant amounts of MoS₂ oxysulfide surface species under HDS reaction conditions.

CONCLUSIONS

Temperature-programmed sulfiding (TPS) appears to be a sensitive technique for study of sulfiding. It gives information on the sulfiding rate and the sulfiding mechanism as a function of temperature.

1. Sulfiding of bulk compounds (MoO₃, MoO₂) occurs at high temperatures in comparison with MoO₃/Al₂O₃ catalysts. Sulfiding of MoO₃ to MoO₂ occurs by H₂S at ca. 650 K. Sulfiding of MoO₂ to MoS₂ occurs at much higher temperatures. This reaction seems to be hindered severely due to H₂S diffusion limitations. Metallic Mo can be an intermediate in MoO₂ sulfiding.

2. Sulfiding of MoO₃/Al₂O₃ catalysts takes place at very low temperatures, in comparison with reduction of these cata-

lysts in TPR. A 4.5 atoms/nm² catalyst can be sulfided completely even at ca. 500 K by selecting a sufficiently low heating rate.

3. Sulfiding appears to be completed at ca. 1100 K in all cases. Nevertheless, the S/Mo ratio after TPS is always below 2 (1.4–1.9, depending on Mo content) pointing to limited formation of MoS₂.

4. Three different sulfiding regions can be discerned: low-temperature sulfiding (<500 K), reduction of elemental sulfur (at ca. 500 K), and high-temperature sulfiding (>500 K).

5. For the low-temperature sulfiding a mechanism is proposed. The dominant reaction is O–S exchange on Mo(VI) ions. Subsequently reduction takes place to Mo(V) and Mo(IV) by rupture of Mo–S bonds, with production of elemental sulfur. This sulfur is reduced to H₂S at ca. 500 K catalytically. Therefore H₂S predominates in low-temperature sulfiding, while H₂ plays only a minor role.

6. An increase of Mo content leads to sulfiding at somewhat lower temperature. However, the influence of Mo content on reduction (TPR) is much more significant. This is explained by detailed consideration of the heterogeneity concept. The covalency and polarizability of Mo–O and Mo–S bonds are introduced as essential concepts.

7. The H₂O content of the catalysts influences sulfiding drastically. Wet catalysts sulfide at very low temperatures (typically 400–500 K), while dried catalysts sulfide at much higher temperatures (typically 600–700 K). H₂O affects the structure of the oxidic catalyst in a reversible way. The influence of H₂O on sulfiding is explained by the assumption of catalysis of sulfiding by Brønsted acid sites. Control of H₂O partial pressure might improve large-scale presulfiding operations by prevention of hot spots.

8. The product of sulfiding up to ca. 500 K might well be a monolayer similar to the oxidic precursor. This monolayer MoS₂ can exist on steric grounds and is represented

tentatively as chains of Mo(IV) oxysulfide species.

ACKNOWLEDGMENTS

This study was supported by the Netherlands Foundation for Chemical Research (SON) with financial aid from the Netherlands Organization for the Advancement of Pure Research (ZWO). Thanks are due to Dr. B. Koch and W. Molleman (University of Amsterdam) for the XRD measurements and to Dr. Ir. V. H. J. de Beer (Eindhoven University of Technology) for his helpful discussions.

REFERENCES

1. Massoth, F. E., "Advances in Catalysis," Vol. 27, p. 265. Academic Press, New York, 1978.
2. Gates, B. C., Katzer, J. R., and Schuit, G. C. A., "Chemistry of Catalytic Processes," Chap. 5. McGraw-Hill, New York, 1979.
3. Seshadri, K. S., and Petrakis, L., *J. Catal.* **30**, 195 (1973).
4. Massoth, F. E., *J. Catal.* **30**, 204 (1973).
5. Thomas, R., van Oers, E. M., de Beer, V. H. J., Medema, J., and Moulijn, J. A., *J. Catal.* **76**, 241 (1982).
6. Topsøe, H., Clausen, B. S., Candia, R., Wivel, C., and Mørup, S., *J. Catal.* **68**, 433 (1981).
7. Clausen, B. S., Topsøe, H., Candia, R., Villadsen, J., Lengeler, B., Als-Nielsen, J., and Christensen, F., *J. Phys. Chem.* **85**, 3868 (1981).
8. Seshadri, K. S., Massoth, F. E., and Petrakis, L., *J. Catal.* **19**, 95 (1970).
9. Massoth, F. E., *J. Catal.* **36**, 164 (1975).
10. de Beer, V. H. J., Bevelander, C., van Sint Fiet, T. H. M., Werter, P. G. A. J., and Amberg, C. H., *J. Catal.* **43**, 68 (1976).
11. Nag, N. K., Fraenkel, D., Moulijn, J. A., and Gates, B. C., *J. Catal.* **66**, 162 (1980).
12. Massoth, F. E., and Kibby, C. L., *J. Catal.* **47**, 300 (1977).
13. Gissy, H., Bartsch, R., and Tanielian, C., *J. Catal.* **65**, 150 (1980).
14. Riddick, F. C., and Peralta, B., Union Oil Company of California, U.S. Patent 4213850 (1980).
15. Hallie, H., *Oil Gas J.*, p. 69. Dec. 20, 1982.
16. Gissy, H., Bartsch, R., and Tanielian, C., *J. Catal.* **65**, 158 (1980).
17. Thomas, R., de Beer, V. H. J., and Moulijn, J. A., *Bull. Soc. Chim. Belg.* **90**, 1349 (1982).
18. Medema, J., van Stam, C., de Beer, V. H. J., Konings, A. J. A., and Koningsberger, D. C., *J. Catal.* **53**, 386 (1978).
19. Gautherin, J. C., Le Boete, F., Colson, J. C., *J. Chim. Phys.* **71**, 771 (1974).
20. Zabala, J. M., Grange, P., and Delmon, B., *C. R. Acad. Sci. Ser. C* **279**, 725 (1974).

21. Grange, P., *Catal. Rev.* **21**, 135 (1980).
22. Arnoldy, P., van den Heijkant, J. A. M., de Bok, G. D., and Moulijn, J. A., unpublished results.
23. Arnoldy, P., de Jonge, J. C. M., and Moulijn, J. A., to be published.
24. Giordano, N., Bart, J. C. J., Vaghi, A., Castellan, A., and Martinotti, G., *J. Catal.* **36**, 81 (1975).
25. Okamoto, Y., Tomioka, H., Katoh, Y., Imanaka, T., and Teranishi, S., *J. Phys. Chem.* **84**, 1833 (1980).
26. Saur, O., Chevreau, T., Lamotte, J., Travert, J., and Lavalley, J. C., *J. Chem. Soc., Faraday Trans. 1* **77**, 427 (1981).
27. Ruetten, F., and Ludeña, E. V., *J. Catal.* **67**, 266 (1981).
28. Diemann, E., and Müller, A., *Coord. Chem. Rev.* **10**, 79 (1973).
29. Wildervanck, J. C., and Jellinek, F., *Z. Anorg. Allg. Chem.* **328**, 309 (1964).
30. Khulbe, K. C., and Mann, R. S., *J. Catal.* **51**, 364 (1978).
31. Rode, E. Y., and Lebedev, B. A., *Russ. J. Inorg. Chem.* **6**, 608 (1961).
32. Tsigdinos, G. A., *Top. Curr. Chem.* **76**, 65 (1978).
33. Declerck-Grimée, R. I., Canesson, P., Friedman, R. M., and Fripiat, J. J., *J. Phys. Chem.* **82**, 885 (1978).
34. Konings, A. J. A., Brentjens, W. L. J., Koningsberger, D. C., and de Beer, V. H. J., *J. Catal.* **67**, 145 (1981).
35. Bachelier, J., Tilliette, M. J., Duchet, J. C., and Cornet, D., *J. Catal.* **76**, 300 (1982).
36. Duchet, J. C., van Oers, E. M., de Beer, V. H. J., and Prins, R., *J. Catal.* **80**, 386 (1983).
37. Kiviat, F. E., and Petrakis, L., *J. Phys. Chem.* **77**, 1232 (1973).
38. Segawa, K. I., and Hall, W. K., *J. Catal.* **76**, 133 (1982).
39. Shell Internationale Research Maatschappij, Dutch Patent 7315573 (1973).
40. Fransen, T., van der Meer, O., and Mars, P., *J. Phys. Chem.* **80**, 2103 (1976).
41. de Beer, V. H. J., and Schuit, G. C. A., in "Preparation of Catalysts" (B. Delmon, P. A. Jacobs, and G. Poncelet, Eds.), p. 343, Elsevier, Amsterdam, 1976.
42. Dufaux, M., Che, M., and Naccache, C., *J. Chim. Phys.* **67**, 527 (1970).
43. Schuit, G. C. A., and Gates, B. C., *AIChE J.* **19**, 417 (1973).
44. Millmann, W. S., Crespín, M., Cirillo Jr., A. C., Abdo, S., and Hall, W. K., *J. Catal.* **60**, 404 (1979).
45. Hall, W. K., and Lo Jacono, M., in "Proceedings, 6th International Congress on Catalysis, London, 1976" (G. C. Bond, P. B. Wells, and F. C. Tompkins, Eds.), p. 246. The Chemical Society, London, 1977.
46. Knözinger, H., and Jeziorowski, H., *J. Phys. Chem.* **82**, 2002 (1978).
47. Cheng, C. P., and Schrader, G. L., *J. Catal.* **60**, 276 (1979).
48. Schrader, G. L., and Cheng, C. P., *J. Catal.* **80**, 369 (1983).
49. Pauling, L., "The Nature of the Chemical Bond," 3rd ed., (a) p. 514 and (b) p. 444. Cornell Univ. Press, Ithaca, New York, 1960.
50. Arnoldy, P., van den Heijkant, J. A. M., and Moulijn, J. A., to be published.